International Journal of Sediment Research 31 (2016) 299–310

Contents lists available at ScienceDirect

International Journal of Sediment Research

journal homepage: www.elsevier.com/locate/ijsrc

Original Research

Simulating bed evolution following the Barlin Dam (Taiwan, China) failure with implications for sediment dynamics modeling of dam removal

Hsiao-Wen Wang [a,*], Desiree Tullos [b], Wei-Cheng Kuo [a]

[a] Department of Hydraulic and Ocean Engineering, National Cheng Kung University, Taiwan, 701, China
[b] Department of Biological and Ecological Engineering, Oregon State University, Corvallis OR 97331, USA

ARTICLE INFO

Article history:
Received 24 November 2013
Received in revised form
2 December 2014
Accepted 7 January 2015
Available online 10 November 2015

Keywords:
Dam removal
Modeling
Sediment dynamics
Channel evolution
Taiwan, China

ABSTRACT

The failure of the Barlin Dam in Taiwan, China offers an important case study for evaluating concepts in modeling the rapid erosion and channel recovery following intentional and unplanned dam removals. We present a modeling effort that applied a 1D and quasi-2D uncoupled hydraulics and sediment model (NETSTARS) to evaluate how discretization and parameterization influence thefitofbed elevationpredictions to observations following dam failure. Our analysis evaluated the model sensitivity to sediment transport function, active layer thickness, and number of stream tubes used to define the cross-section. Results indicate that a) the model is more sensitive to active layer thickness and sediment transport function than to the number of stream tubes, b) development of dam removal models are likely to benefit from varying the active layer thickness in time, and c) increased lateral discretization does not appear to improve model fit in the steep and rapidly changing river environment at our site. We conclude with discussion on differences between, identifying the need for, and general use of 1D, quasi-2D, and fully 2D models in dam removal and failure analysis.

1. Introduction

The fate of sediment released following dam removals has been the focus of increasing study as dams reach the end of their working life and connectivity is increasingly prioritized for river restoration purposes. Much of this research has emphasized field monitoring (e.g. Doyle et al., 2002; Kibler et al., 2011; Major et al., 2012) of the rates of and patterns in erosion and deposition following the pulse release of sediment with dam removal. Numerical and physical modeling studies are also increasing undertaken (Cui et al., 2006; Cantelli et al., 2007; Wells et al., 2007; Cui & Wilcox, 2008; Downs et al., 2009; Konrad, 2009) in an effort to advance understanding on dam removal impacts and the sediment dynamics of sediment pulses. These numerical modeling efforts include both the development of models specific to dam removal (Cui et al., 2006; Cantelli et al., 2004) and the application of general hydraulic-sediment transport models, including one-dimensional (1D) (Chang, 2008; Rathburn & Wohl, 2003; Wells et al., 2007; Tullos et al., 2010) and quasi-2D and 2D models (Rathburn & Wohl, 2003) to analyze sediment dynamics of dam removal.

However, as many of these efforts have shown, numerical modeling of sediment pulses is a particularly difficult problem (Wu, 2004), in part because channel response depends on a number of spatially and temporally variable site characteristics (Tullos & Wang, 2014) that can be difficult to estimate with certainty and to represent accurately in numerical models. For example, the volume and caliber of sediment stored behind a dam and contributed from upstream of the site can strongly influence channel response to sediment pulses (Pizutto, 2002; Lisle et al., 2001). However, measurements of sediment characteristics and transport rates, which are needed as input or boundary conditions for sediment models, can be logistically challenging and expensive to collect (Emmett, 1980; Hubbell, 1987), highly variable in space and time (Wilcock et al., 1996; Hubbell, 1964; Gomez, 1991), and generally prone to error (McLean, 1985; Hubbell, 1987). These uncertainties are compounded when applied in the estimation of sediment transport capacity from the various functions available (Gomez & Church, 1989; Barry et al., 2004). Furthermore, the

* Corresponding author.
E-mail address: whw82@mail.ncku.edu.tw (H.-W. Wang).

http://dx.doi.org/10.1016/j.ijsrc.2015.01.004
1001-6279/

temporal and spatial variability of some site characteristics can also be difficult to represent in hydraulic models. For example, the depth and erodibility of the underlying geologic material can be highly variable in space and time and have been shown to influence channel gradient and transport capacity (Goode & Wohl, 2010). Yet, direct measurements of bedrock exposure and incision are uncommon in field surveys (Stock et al., 2005) and bedrock depths are commonly represented as uniform in hydraulic models. In addition, lateral variability in velocities and shear stresses produce local patterns in erosion and deposition (Wilcock et al., 1996). While some authors (Downs et al., 2009) have reasonably argued that 1D numerical simulation of reach-level channel changes is the most appropriate scale for modeling channel responses to sediment pulses, others (Ferguson & Church, 2009) are critical of the ability of 1D models to represent the spatial and temporal variability of sediment dynamics across and down rivers. However, for all of these ways in which modeling may poorly represent reality, it is unclear how important any of omitted details are on predictions of erosion and deposition.

Thus, the broader goal of this effort is to investigate how different representations of channel variability influence fit of post-hoc modeling to field observations of the Dahan River, Taiwan, China following the failure of Barlin Dam. More specifically, the objectives of this analysis were to a) estimate fit ofa 1D model and of increasing discretization of quasi-2D simulations, based on the hypothesis that quasi-2D simulations better represent lateral variability in erosion and deposition, and b) evaluate sensitivity of the 1D and quasi-2D models to the selection of sediment transport functions and to the treatment of temporal variability in the depth of the active layer thickness. The results contribute to ongoing discussion regarding strategies for modeling dam removal sediment dynamics, based on a case study with an exceptionally large (8.3 million m^3over15 months) pulse of sediment released during a large typhoon in 2007.

In this paper, we briefly review the Barlin Dam failure, report fit of simulated and observed longitudinal profiles, investigate differences in patterns and magnitudes of erosion and deposition between the simulated and observed profiles and cross sections, present results of a sensitivity analysis, and discuss implications for modeling sediment dynamics of dam removal.

We report results of sediment modeling associated with the pulse release of sediment associated with the failure of the Barlin Dam on the Dahan River, Taiwan, China. Barlin Dam, constructed in 1977, was a 38-m-high concrete gravity dam with rotary-arm gates. It was among the largest of over 100 sediment retention structures built in the catchment to reduce erosion and sediment delivery to Shihmen Reservoir, which is located approximately 40 km downstream and generates municipal, industrial, and irrigation water, hydropower, and flood protection benefits. Barlin's initial storage capacity of 10.5 million $m^3$was filled with sediment by 2003 and bedload material was passed over the dam. In 2004, a 'defense dam' constructed for energy dissipation immediately downstream of Barlin Dam was damaged due to undercutting, which allowed incision to propagate upstream to the base of Barlin Dam. Barlin Dam then failed during Typhoon WeiPa in September 2007, a roughly 5-year return event with an estimated peak discharge of 225 cms (Tullos & Wang, 2014).

The Dahan River drains a geologically-active 1,163 km^2 basin in the northern Central Range of Taiwan, China (Fig. 1). Steep hillslopes (exceeding 55% in over two-thirds of the drainage basin), fractured bedrock, and intense monsoonal precipitation (over 2000 mm annually), result in frequent landsliding and sediment yields that are among the highest in the world (Milliman & Syvitski, 1992; Huang, 1994; Dadson et al., 2003). At the Yufeng gauging station, located approximately 22 km upstream of the former Barlin Dam site (Fig. 1), the long-term (1957–2002) suspended sediment yieldis 0.583 million tons per year, based on rating curves developed by Shihmen Reservoir Administration

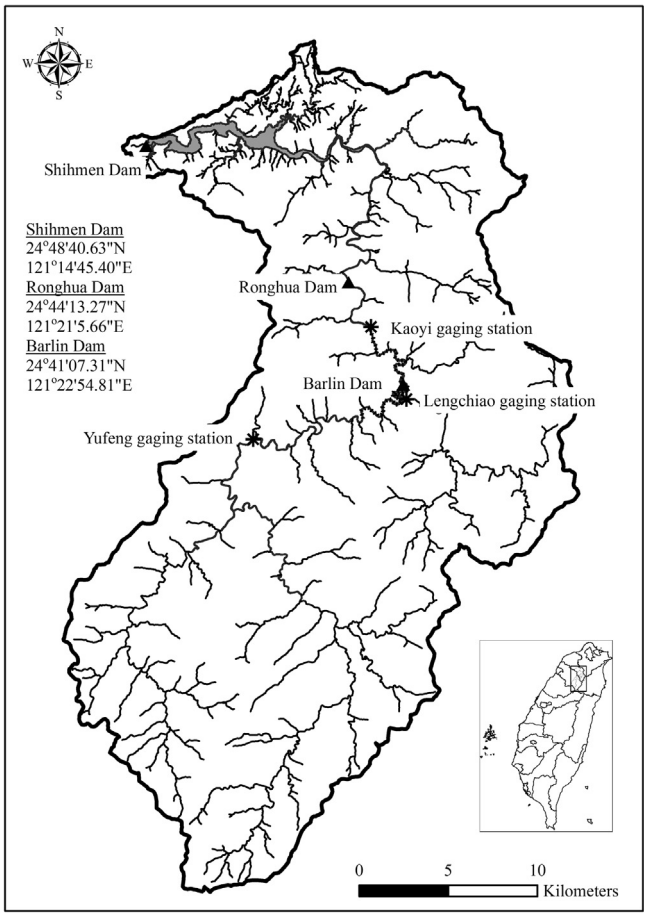

Fig. 1. Map of the Dahan River catchment in Taiwan, China. The frame indicates the simulation reach. Inset: location map of Dahan River basin.

(2006). With suspended load comprising approximately 70% of the total load (Dadson et al., 2003), the average annual bedload at the Yufeng station is estimated to be 0.251 million metric tons.

Within the study reach, defined by the former reservoir extending 4.8 km upstream and 5.2 km downstream of the former dam site, the Dahan River is a forced-meander river with bedrock locally exposed along the margins of the river. The valley gradient is 0.01 and sinuosity is approximately 1.6. Prior to dam failure in 2006, the mean reservoir width was 116 m while the mean width of the downstream channel was 155 m, owing to differences in valley configurations of the two reaches. Substrate varied between years as a function of landslide inputs and the frequency and magnitude of high flows. In 2007, prior to dam failure, both the reservoir and downstream substrates were dominated by very fine gravel, with mean D_{50} of 3.9 mm and 2.1 mm, respectively. A major tributary (Sankuan Creek, catchment area = 392 km^2) enters the Barlin impoundmentapproximately 1500 m upstream of the dam (Fig. 1). While we have no quantitative information about the depth of bedrock in our study reach, the authors observed bedrock exposure along the margins and lining the valley walls near the dam, and that the exposure varied in space.

2. Methods

2.1. Observed erosion and deposition

We analyzed fifty cross-sections from bathymetric field surveys conducted by the Taiwan Water Resources Agency (WRA) on

reaches 4.8 km upstream and 5.2 km downstream of the Barlin Dam. Surveys were conducted prior to dam failure in September 2007 and following dam failure in December 2007 and December 2008. Bathymetry for the September 2007 survey was collected as cross-sections at approximately 200 m spacing. The post-failure surveys were conducted with the intent of generating contour maps, resulting in an irregular sampling scheme with typical point densities of 1 point per 290 m^2 and with emphasis on defining depositional features and the main channel at baseflow. All surveys were conducted by total station and only in wadeable areas. This wadeable survey approach precluded surveying the thalweg in a few areas, but the maximum gap in cross-section measurements for the deepest parts of the channel appears to be small (<2 m) across the entire study area. Because topographic surveys before dam failure were based on cross-sections, we used the contour-based surveys conducted after dam failure to generate elevational surfaces from which cross-sections were cut at the locations of the pre-failure cross-sections. These cross-sections were used as inputs to define the model bathymetry and to construct a longitudinal profile, based on cross-section thalweg elevations, and to evaluate model fit to observations as described in Section 2.2.3.

2.2. Modeled bed elevation changes

2.2.1. Overview of modeling computations

We applied the Network of Stream Tube Model for Alluvial River Simulation (NETSTARS-Lee et al., 1997) model to simulate bed elevation changes following the Barlin Dam failure. NETSTARS is a quasi-2D, finite difference, uncoupled hydraulic and sediment routing model that defines a reach by stream tubes (Lee et al., 2003; Yang, 2008) to simulate hydraulic conditions and bed elevations. The model applies the 1D energy and continuity equations to calculate stage and discharge under steady flow conditions, and solves the 1D St Venant momentum and continuity equations for unsteady flows. The governing equations for sediment routing consist of a sediment continuity equation, a convection-dispersion equation for suspended sediment movement, and a number of bed load and total load transport functions, accounting for bed sorting, armoring, and transport of non-uniform sediments. NETSTARS applies the concept of stream tubes, imaginary tubes bounded by streamlines, to represent lateral variability in hydraulics and morphodynamics, though no convective and diffusive exchange occurs across the streamlines. Simulations within each tube are 1D, raising and lowering the bed elevations associated with scour and deposition in each tube. Hence, the model can represent the lateral variations of elevations across the channel, but cannot simulate secondary currents, recirculating flow, or lateral erosion of streambanks and terraces.

NETSTARS computations proceed by first calculating the hydraulic characteristics of the full channel. With a horizontal water surface elevation across the cross section, the channel is then divided, and updated at each time step, into the user-defined number of stream tubes based on the principle of equal conveyance within a tube. While the lateral location of each stream tube is defined by the model at each time step, the length of each stream tube is defined by our 200-m-spaced cross-sections. The bed elevation computations are then performed in each tube and each time step.

2.2.2. Initial and boundary conditions and modeling parameters

We used fifty surveyed cross-sections of the pre-failure channel as the initial bathymetry. This model was used to simulate the bed elevations for December 2007, a period of rapid erosion of reservoir sediments, henceforth referred to as “Period 1.” We then used the observed bathymetry from the December 2007 survey as the initial bathymetry to simulate bed elevations for December 2008. This year, henceforth referred to as “Period 2,” wasa period of slower channel response that occurred after a continuous gradient was established between the upstream and downstream reaches during Period 1.

One grain size distribution data set was used to represent the bed sediment within the entire study reach as the initial riverbed substrate, based on the average distribution (Fig. 2) of eight 1 m^3 bulk samples (WRA, 2007; Fig. 2). Manning’s roughness coefficient, n, varied by cross sections and was set as 0.03–0.06 based on field observations by the authors and by WRA (2008b). Due to the data availability (Agriculture Engineering Research Center, 2009), we used hourly flow discharge records for September 2007 to December 2007 (Fig. 3a), and daily flow discharge records for December 2007 to December 2008 (Fig. 3b) from the Yufeng gauging station (Fig. 1), as the upstream boundary condition. Water stage from the Kaoyi gauging station(Fig. 1) were used as the downstream boundary condition, and discharge records from Lengchiao gauging station were used as the flow boundary condition for the tributary entering the reservoir just above the former dam (Fig. 1). Rating curveswere used as the upstream boundary conditions for suspended sediment transport routing.

$$Q_s = 0.92 * Q^{1.889} (R^2 = 0.877) \text{ for Yufeng gauging station} \quad (1)$$

$$Q_s = 1.13 * Q^{1.908} (R^2 = 0.679) \text{ for Lengjiao gauging station} \quad (2)$$

Q_s is the sediment discharge in million tons/day, and Q is the discharge in cms. These rating curves are based on 1440 suspended sediment samples,collected 20–30 times per year from 1957 to 2002. NETSTARS provides two options to estimate total load of sediments. One option directly estimates the total sediment load, while the other option results from the summation of separate estimates of bed load and suspended load (Lee et al., 2003). For sediment transport functions dealing with total load, such as Ackers and White (1973) and Yang (1973), the total load is calculated based on the input discharge records and the rating curves given above (Eqs. 1, 2). For sediment transport functions only treating bedload, such as Meyer-Peter and Muller (MPM, 1948), Rouse number is used to distinguish between suspended load and bedload.

2.2.3. Model calibration and evaluation

Rather than applying the zeroing process outlined by Cui et al. (2006), we simulated the model for Period 1 under a range of the following parameters: sediment function, number of stream tubes, and active layer thickness. The pre-failure bathymetry (September 2007) was used as the initial geometry to simulate the bed elevations for the three months post-failure for Period 1, through

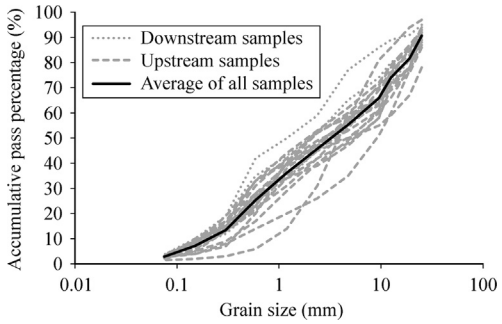

Fig. 2. Grain size distribution of study reach sediments. Grey lines reflect results of eight field-sieved 1m^3 bulk samples from both upstream and downstream of Barlin Dam prior to failure. The dark black line, the average of all samples within the 10-km study reach, was used as the grain size distribution for all cross sections in the model.

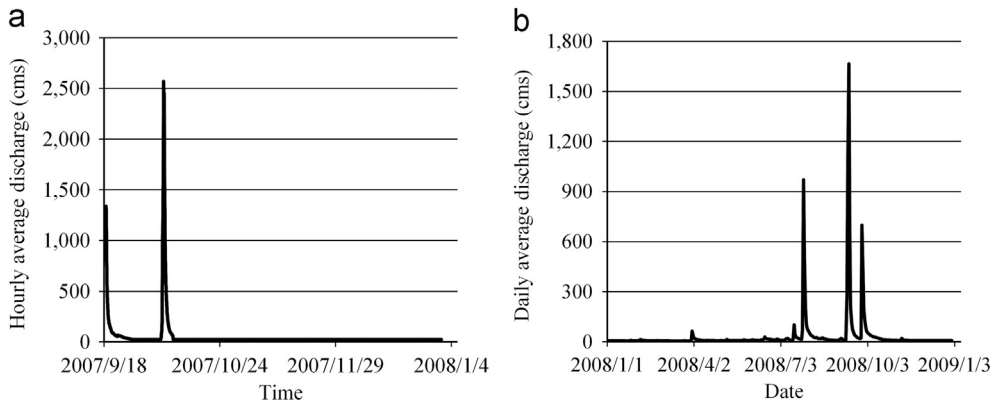

Fig. 3. Upstream boundary conditions for two simulation periods: (a) hourly flow discharge from September 2007 to December 2007, for Period 1, and (b) daily flow discharge from December 2007 to December 2008, for Period 2.

which sediment function, number of stream tubes, and active layer thickness were evaluated for their effect on model fit. Model fit was then evaluated using the Root Mean Square Error (RMSE) and the normalized RMSE (error-min. error)/(max. error-min. error) based on the thalweg elevations (see Section 2.2.4 Sensitivity Analysis). The scenario with the lowest RMSE for the Period 1, as the calibration period, to all model scenarios is referred to the calibrated scenario, and the tuned parameters for this scenario were then applied to all model configuration scenarios. The three-month post-failure observed bathymetry (December 2007) was then used as the initial geometry for Period 2, representing the model verification period.

We also evaluated the model based on comparison of observed and modeled volumes of scour and fill for the calibrated scenario. The volume of eroded and deposited material was estimated by calculating differences between post-failure bed elevations and the September 2007, pre-failure bed elevations. Elevations were linearly interpolated between cross-sections along the reaches upstream and downstream of the former dam and volume changes were calculated as the product of the differencein area between the two survey periods and longitudinal distance between cross-sections.

2.2.4. Sensitivity analysis

We performed a sensitivity analysis to evaluate model responsiveness and fit to a) increasing discretization of the channel cross section by representing the channel as one, three, and five stream tubes; b) varying active layer thickness; and c) varying the sediment transport function. We did not evaluate the sensitivity of the model to field measurements, but refer the reader to references (Cui et al., 2006; Chang et al., 1993) for analysis of sediment model sensitivity to grain size distribution, discharge/velocity, roughness/resistance coefficients, sediment supply, active layer thickness, and other parameters, such as attrition rate (Downs et al., 2009). We also did not investigate parameter uncertainty, though we refer readers to work (Ruark et al., 2011) highlighting important issues associated with differing parameter uncertainties in erosional and depositional environments.

We applied three sediment transport equations (Yang, 1973; Ackers & White, 1973; MPM, 1948) for this analysis, selected to evaluate how conditions (e.g. grain size, gradient, planar or a range of bedforms) under which the equations were developed may influence accuracy in predicting bed elevation changes.

We also evaluated the depth of the active layer thickness as two, four, and six times the size of the largest grain (Dmax), as it can exert an important influence on the accuracy of bed elevation predictions (Rulot et al., 2012; Struiksma, 1999; Tullos et al., 2010). According to the bed composition accounting procedure proposed by Bennett and Nordin (1977), the active layer is a surficial layer that is well-mixed and available for mobilization. It represents all the sediment that is available for transport at each time step. In NETSTARS, the thickness of the active layer is defined by the user as proportional to the geometric mean of the largest size class containing at least 1 percent of the bed material at that location. Active layer thickness is also related to the time step duration. As sediment was eroded and deposited following dam failure, it is expected that the active layer thickness varied with time. We expected that a larger active layer thickness during Period 1 would better represent the dramatic erosion immediately after dam failure, but result in overestimating erosion in the reservoir during Period 2. We thus anticipated that the importance of this factor would vary across the two simulation periods.

3. Results

3.1. Observed channel changes

As reported in Tullos and Wang (2014), dam failure resulted in rapid erosion and downstream transport of sediment from the former reservoir. Within three months, 3.6million m^3 of sediment had eroded from the reservoir, and after fifteen months, 8.3 million m^3hadbeen transported downstream. The mean bed elevation changes include about 8 m of incision upstream of the dam, as well as aggradation to maximum depths of over 5.5 m over 5 km of the riverbed downstream of the dam (Fig. 4). The reservoir gradient increased from 0.006 in 2007 to 0.010 in 2008 over the 5-km reach upstream of the dam. The gradient over a 5-km reach downstream of the dam changed very little, from 0.009 to 0.010, over the same time period. See Tullos and Wang (2014) for more detailed analysis of geomorphic recovery following the Barlin Dam failure.

3.2. Modeled channel changes

3.2.1. Model fit to thalweg profile across space and time

Before mobile-bed modeling, the flow hydraulics needs to be computed accurately. The measured water surface elevations at Kaoyi gaging station during Typhoon Wipha (2007/9/18 15:00–9/23 23:00) and Typhoon Krosa (2007/10/5 0:00–10/10 9:00) were used to calibrate and verify the simulated water surface elevations. The comparison of simulated and observed water stage (Fig. 5) indicates that the model predicted the water surface elevation reasonably well, with a RMSE of 0 m and 0.75 m for the calibration and verification, respectively.

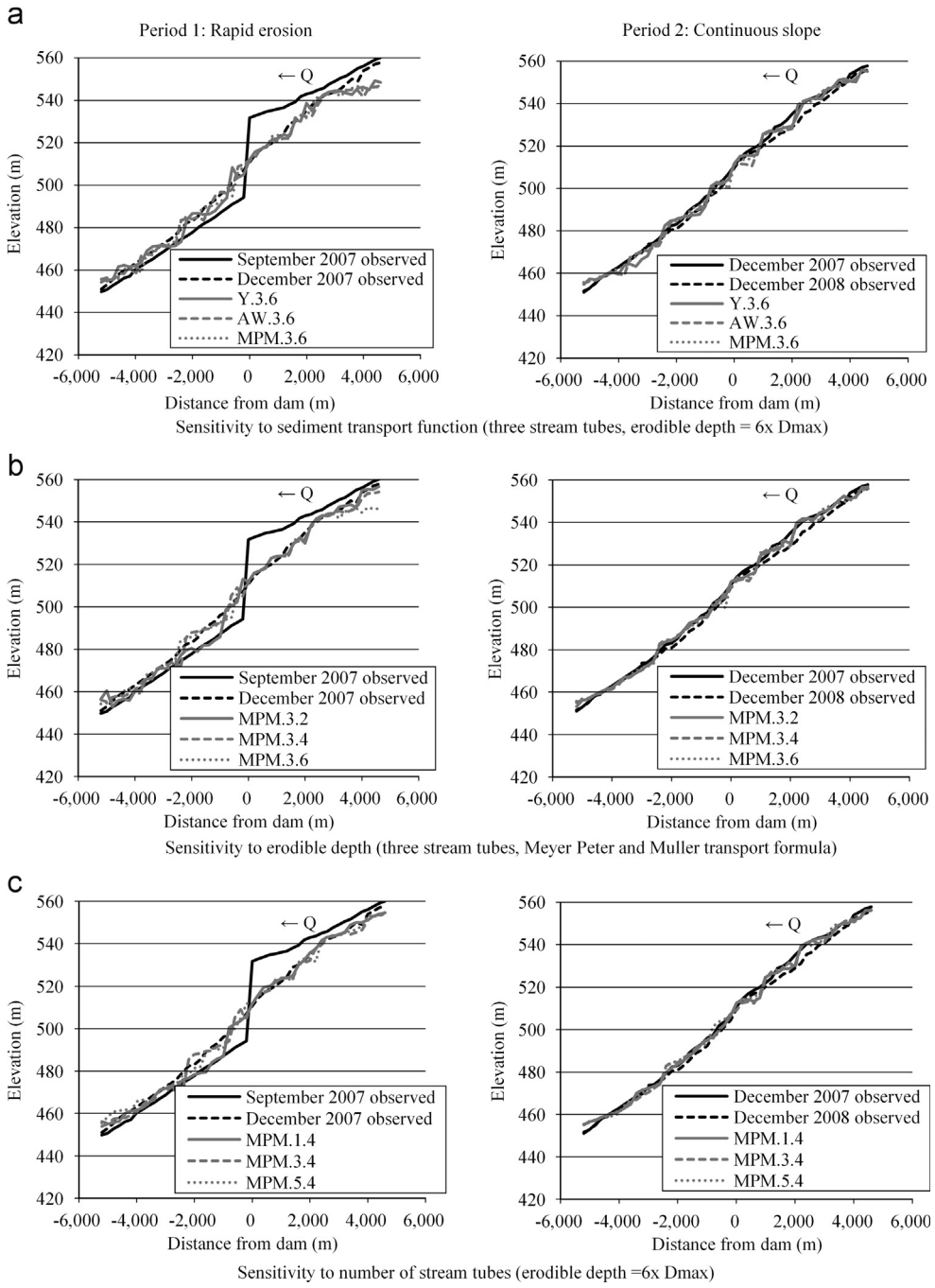

Fig. 4. Sensitivity of simulated longitudinal profiles to a) sediment transport formula, b) active layer thickness, and c) number of stream tubes for two simulation periods: September 2007–December 2007 (left) and December 2007–December 2008 (right). The arrow indicates the flow direction.

For the bed variation, based on the RMSE values and simulated thalweg profiles, the MPM function with three stream tubes and an active layer thickness of four times the Dmax best fit the observed changes in the Dahan River during Period 1, with the lowest calibrated error of 1.46 m relative to the other model scenarios. While there does not appear to be any trend in model error with distance from the dam in the upstream or downstream directions for either time period (Fig. 6c, d), the degree of model fit does vary across the two simulation periods.

Overall, errors were nearly always higher during Period 1 than in Period 2. The largest errors were generally associated with simulating sediment transport with the Ackers and White (1973) and Yang (1973) functions, particularly during Period 1. During Period 2, the model calibrated for Period 1, using the MPM function, the medium active layer thickness and three stream tubes, was not the model configuration with the lowest error. Instead, model error was lowest for MPM transport function and one stream tube, regardless of the active layer thickness, during Period 2 when channel changes were smaller and slower than Period 1. Because the MPM transport function appears to produce the most accurate bed elevations and for brevity, all subsequent results will eliminate results from the other two sediment transport functions.

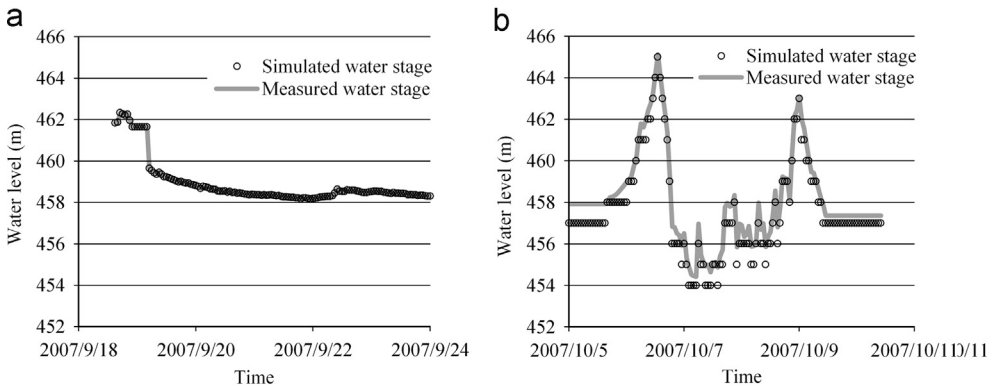

Fig. 5. The comparison of simulated and measured water stage variation with time at Kaoyi gaging station: (a) calibration (b) verification.

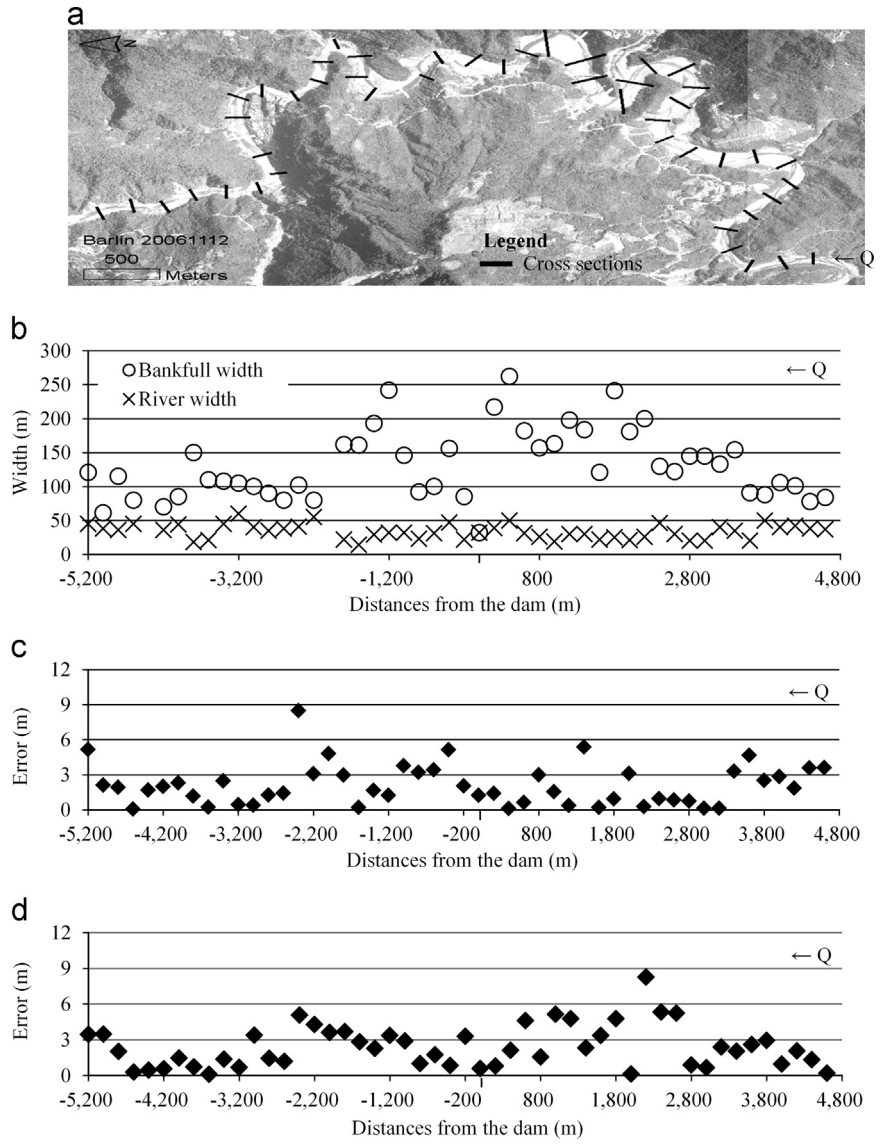

Fig. 6. Model errors with distance from the dam against channel width: (a) locations of analyzed cross-sections on an aerial photo of 2006, (b) channel widths of each section, (c) errors (thalweg difference) between simulated and surveyed profiles for Period 1 of the calibrated scenario, MPM.3.4, and (d) errors (thalweg difference) between simulated and surveyed profiles for Period 2 of the calibrated scenario, MPM.3.4. The arrow indicates the flow direction.

Observed and simulated longitudinal profiles (Fig. 4) both demonstrate the better performance of the model in Period 2, as well as where errors appear to be concentrated during Period 1. The observed thalweg profile of Period 2 was more accurately represented by all model configurations than for Period 1. The error during Period 1 was greatest at the most upstream extent of the reservoir and in the downstream reach just below the former dam site. More specifically, model simulations generally fit erosion patterns in the reservoir, but overestimated erosion above 4000 m upstream of the former dam site (Fig. 4a). The overestimation of reservoir erosion at this relatively narrow reach (~75–105 m) may be attributable to the simulated active layer thickness of six times of the Dmax overestimating the amount of material available above the bedrock valley bottom at the site. During Period 2, error in predicted reservoir thalweg elevations was concentrated approximately 2400 m upstream of the dam site. At this location, all model scenarios underestimated reservoir erosion on the order of 5 m (Fig. 4).

In the downstream reach, simulation error for Period 1 (Fig. 4a) was concentrated in a reach that falls between 400 m and 1600 m below the dam site. In this section, most model configurations underestimated deposition by up to 10 m (Fig. 4b). For period 2, the model simulated the thalweg profile similarly well for all model scenarios, with no areas of concentrated error.

3.2.2. *Model fit at cross-sections with varying streamtubes*

Our hypothesis that model fit to observations within an individual cross-section would increase with increasing number of stream tubes was not confirmed. Field surveys indicate that the cross-sections eroded or deposited sediment relatively uniformly across the channel (Figs. 7 and 8). Some of the stream tube configurations simulated more variability and/or more net erosion or deposition than was observed, though the number of stream tubes that best fit the uniformity and volume of erosion or deposition varied by cross section. In evaluating all of the simulated cross-sections, we did not see any evidence of a single “best” number of stream tubes.

Instead, the number of stream tubes needed to simulate any individual cross-section appears to be related to the width and location of the reach. For example, approximately 400 m upstream of the former dam, the active channel prior to dam failure was shallow and around 165 m wide (Fig. 7a). At this location, the cross-section uniformly incised during Period 1, a response that was relatively well-matched by simulations with one stream tube, but not with three and five streamtubes (Fig. 7a). The incomplete erosion on the inside of the meander, oriented on the left side of the channel, with three and five stream tubes resulted in an underestimate of the volume eroded by approximately one half of the observed erosion (Table 1). During Period 2 (Fig. 7a), the number of stream tubes had minimal effect on the variability at this cross-section 400 m upstream of the dam site. Approximately 1000 m upstream of the former dam site, a 185 m wide, braided section of the channel was simulated with similar accuracy for all stream tube configurations during Period 1 (Fig. 7b). During Period 2, all the three configurations simulated deposition at this location, though the channel was observed to incise during this period (Fig. 7b).

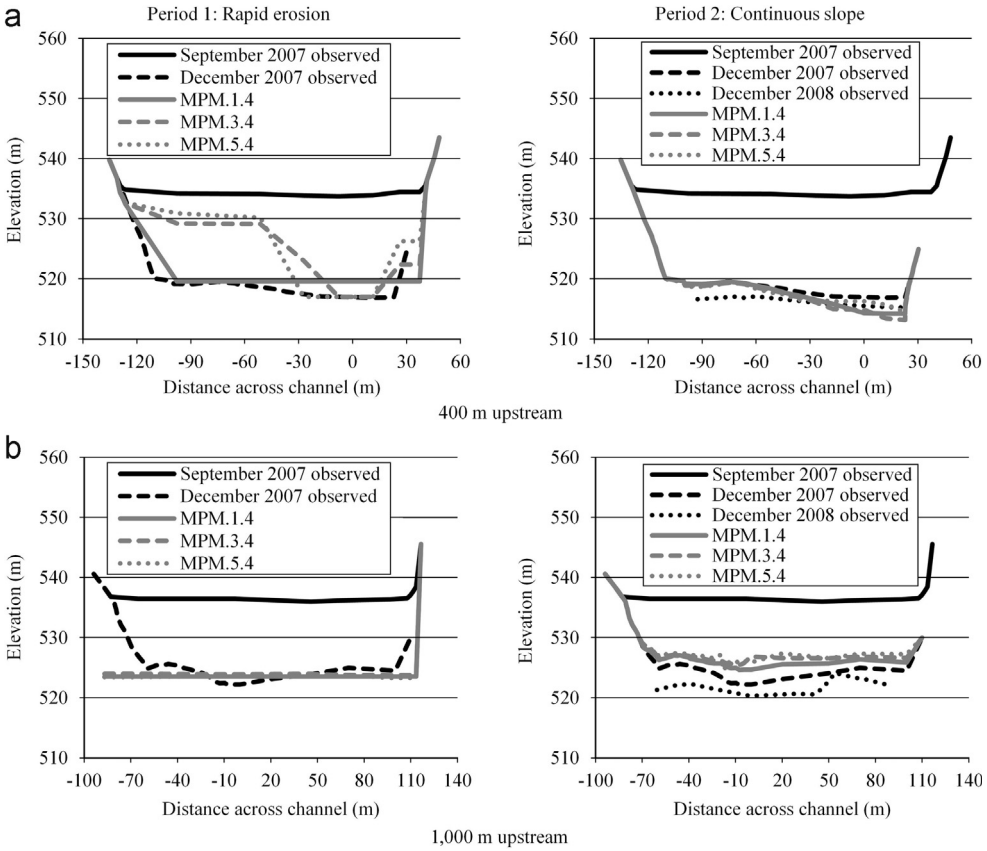

Fig. 7. Selected observed and simulated upstream cross sections. Cross sections are presented for the simulations with active layer thickness of four times the maximum grain size. River left (looking downstream) is oriented on the left of the graph and all cross-sections are adjusted to a zero location that reflects the thalweg in the pre-failure survey.

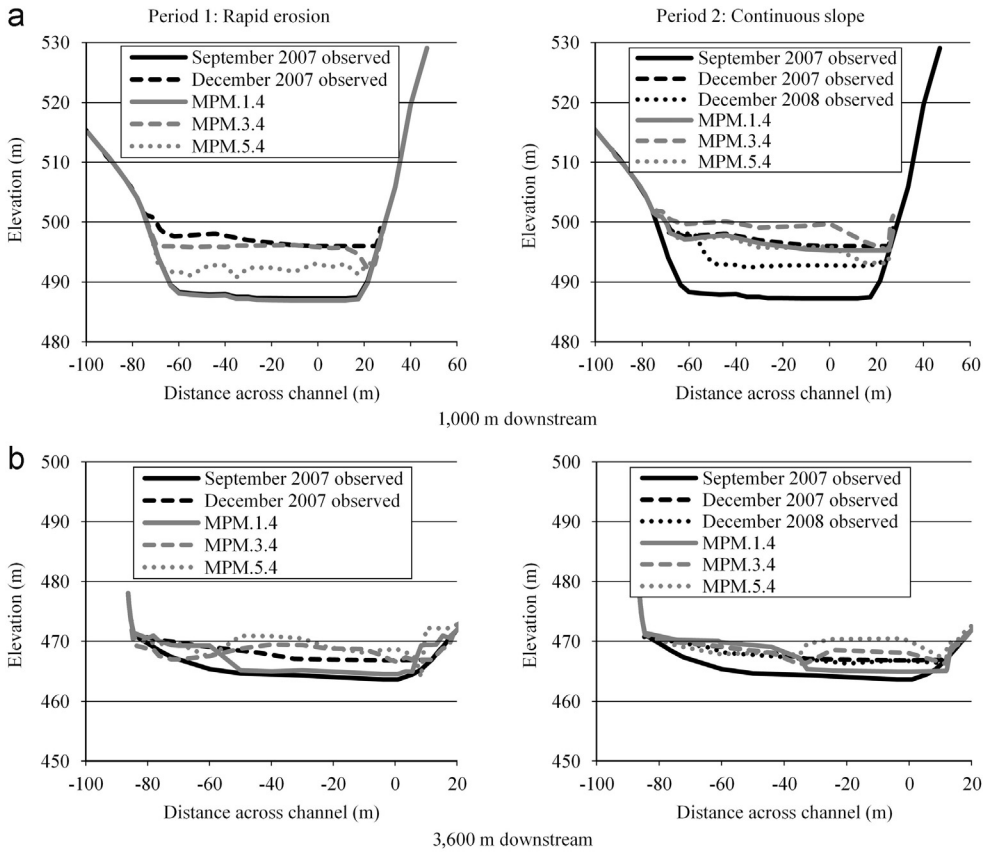

Fig. 8. Selected observed and simulated downstream cross sections. Cross sections are presented for the simulations with active layer thickness of four times the maximum grain size. River left (looking downstream) is oriented on the left of the graph and all cross-sections are adjusted to a zero location that reflects the thalweg in the pre-failure survey.

Table 1
Comparison between modeled volumes of scour and fill for the calibrated scenario (MPM.3.4) and the observations.

Reach	Period 1 September 2007–December 2007			Period 2 December 2007–December 2008		
	Observed volume (m^3)	Simulated volume (m^3)	Error	Observed volume (m^3)	Simulated volume (m^3)	Error
Upstream	−3539573	−5305346	50%	−4828020	175733	−104%
Downstream	2875847	4028284	40%	−496953	−1258273	153%
NET	−663726	−1277062	92%	−5324973	−1082540	−80%

Varying the number of stream tubes also had an effect on model accuracy in the downstream reach. For example, in a narrow (~80 m wide), constrained run approximately 1000 m downstream of the former dam site (Fig. 8a), the single stream tube configuration failed to simulate any of the 10 m of deposition that occurred in the three months following failure. While the three and five stream tube configurations did predict deposition, they both underestimated the amount of deposition that occurred in Period 1. During Period 2, the three-tube configuration simulated further deposition and the other two configurations predicted negligible change at this location, though the channel was observed to incise during this period. At a slightly wider (~100 m) riffle located 3600 m downstream of the former dam (Fig. 8b), the relatively uniform deposition that occurred was not closely simulated for any of the stream tube configurations during Period 1. Some stream tube scenarios (e.g. MPM.3.4, MPM.5.4) overestimated deposition by up to 6 m., while the one-tube configuration (MPM.1.4) underestimated deposition. The fit to observations during Period 2 was better than model fit for Period 1, with a maximum overestimated deposition of up to approximately 3 m (e.g. MPM.5.4). However, while the net error was lower for Period 2, simulations generated variability in the cross-section that was not observed in the field.

Based on the review of these and other simulated cross-sections not presented here, we see no clear patterns in the performance of the different stream tube scenarios, across the different channel unit types (e.g. run, riffle, braided) or channel

widths, to indicate that the quasi-2D model could capture erosion and deposition across the channel better than the 1D model.

3.2.3. Model sensitivity

The ranges of RMSE provide a measure of the sensitivity of the models to combinations of stream tubes, sediment transport function, and active layer thickness. Beginning with the sediment transport functions by holding the active layer thickness at 6 times the Dmax, the variability in RMSE across sediment transport functions was only 0.32 m (NRMSE = 0.13) and 1.38 m (NRMSE = 0.56) for three and five stream tubes, respectively during Period 1 and was 0.1 m (NRMSE = 0.04) and 0.26 m (NRMSE = 0.1) for three and five stream tubes, respectively, during Period 2. Next, we varied the active layer thickness and number of stream tubes while holding the sediment transport function constant by applying only the MPM (1948) formula. Across the three active layer thicknesses, the RMSE variability ranged from 0.81 m (NRMSE = 0.33), 1.04 m (NRMSE = 0.43), and 0.86 m (NRMSE = 0.35) for one, three, and five steam tubes, respectively, during Period 1. During Period 2, the ranges of RMSE variability of active layer thickness are much lower, on the order of 0.19 m (NRMSE = 0.08), 0.12 m (NRMSE = 0.04), and 0.46 m (NRMSE = 0.18), for one, three, and five stream tubes, respectively, during Period 2. Finally, we report ranges of RMSE variability while varying the number stream tubes in simulations with the MPM (1948) transport function. Varying the number of stream tubes resulted in sensitivity ranges that fall between sediment transport functions and erodible depths: RMSE ranges were 0.56 m (NRMSE = 0.23), 0.45 m (NRMSE = 0.19), and 0.95 m (NRMSE = 0.39) for active layer thicknesses of six, four, and two times the Dmax, respectively, during Period 1, and 0.53 m (NRMSE = 0.21), 0.39 m (NRMSE = 0.16), and 0.26 m (NRMSE = 0.11) for active layer thicknesses of six, four, and two times the Dmax, respectively, during Period 2.

This results of sensitivity analysis highlights that the model is sensitive to all three model parameters, though the sensitivity varied with simulation period. For example, the range of RMSE variability was the highest (1.38 m, NRMSE = 0.56) when varying sediment transport functions for five stream tubes during Period 1, indicating high sensitivity to sediment transport functions during the initial stage of rapid erosion. The widest RMSE ranges (1.04 m, NRMSE = 0.43) occurred when varying active layer thicknesses, but only during Period 1. The order of magnitude larger RMSE ranges for the active layer thickness during Period 1 suggests the model is more sensitive to this model parameter during the period of rapid channel change and confirms that varying active layer thickness over time could increase model accuracy. Sensitivity to the number of stream tubes does not vary as much as active layer thickness in two simulation periods. It may instead be related to the width and configuration of the subreach (Section 3.2.2).

3.3. Practical implications of model error

The practical implications of RMSE values are represented by the effects of simulated errors on the volume of reservoir erosion and downstream deposition (Table 1) for the directly calibrated scenario (MPM.3.4). In both the reservoir and downstream reaches during Period 1, the model overestimated channel changes, relative to our observations, by overestimating both reservoir erosion and downstream deposition. The model failed to estimate channel changes during Period 2, with substantial underestimations of reservoir and downstream erosion. These absolute errors illustrate how RMSE values translate into potentially substantial errors in volumes of scour and fill, and that these errors can be larger for the slower response of Period 2 than the rapid change of Period 1. Despite the nearly 20 m of incision for Period 1 and only ~2 m of incision during Period 2 (Fig. 4), the error resulted in substantially different error of 50% and 104% in the upstream reach (Table 1). Practically, such an error may be large enough to influence decision-making regarding acceptability or engineering in a dam removal scenario.

4. Discussion

Numerical modeling of sediment pulses is a particularly difficult problem (Wu, 2004), in part because channel response depends on a number of spatially and temporally variable site characteristics (Tullos & Wang, 2014) that can be difficult to estimate with certainty and to represent accurately in numerical models. The failure of Barlin Dam released a pulse of sediment considerably larger than has occurred at the large majority of intentional dam removals, and thus simulating the channel recovery can shed light on approaches to simulating future dam removals.

While the importance of other factors, such as grain size distribution, discharge/velocity, sediment influx, roughness/resistance coefficients, etc., are also critical in influencing model performance (Downs et al., 2009; Newham et al., 2003; Ruark et al., 2011), in this analysis, we sought to investigate how varying the sediment transport function, active layer thickness, and number of stream tubes influenced model fit to observations. The model appears to be sensitive to active layer thickness and the selected sediment transport functions, as discussed in further detail below, but is not clearly responsive to the number of stream tubes.

4.1. Sensitivity to active layer thickness and sediment transport functions

Variations in the elevations of buried bedrock surfaces can limit the depth of incision and can have an important influence on the accuracy of sediment transport models (Morris & Fan, 1998). It appears that the active layer thicknesssimulating the best fit to observations varies between the two simulation periods, with a thicker layer thickness performing better in Period 1 and a thinner thickness performing better in Period 2. In addition, the model appears to be more sensitive to active layer thickness during Period 1 than during Period 2. This result suggests that collecting field estimates of erodible thickness of bed materials that can limit the extent of bed lowering in the reservoir, when possible, can potentially lead to valuable improvements in simulating sediment dynamics during the period of rapid erosion immediately following dam removal. In addition, because only one set of active layer thickness can be used for simulation in NETSTARS, the spatial variability of active layer thickness was not considered in the model. Because modeling results can be dependent on active layer thickness, advancement of model development capable of incorporating spatial variability for active layer thickness (Yang & Young, 1997) is needed.

Model fit is also sensitive to sediment transport function. Results indicate that the MPM sediment transport function provided the best match to the morphology and other channel features that drive sediment entrainment in the Dahan River. This result illustrates how the features of sediment transport functions, such as input parameters, mathematical formulation, and range of conditions for developing the functions, can be important in simulating the patterns of rapid erosion and longer-term bed changes in this system. This result highlights the need for a deliberate process that identifies the transport function best matched to the local conditions. For example, in a dam removal modeling scenario, measurements of bed and suspended load prior to dam removal are compared to predictions by transport function to select the one that best matches historical deposition and scour (Yang, 2006). However, as bed and suspended load data

are often not available, other techniques (e.g. Simons & Şentürk, 1992; Williams & Julien, 1989) may be employed for justifying the selection of sediment transport function.

4.2. Effects of increasing model discretization

Our modeling scenarios appear to be insensitive to increasing discretization of the channel cross-section, and the 1D simulations performed as well or better than the quasi 2D model for many of the cross-sections. Based on simulations applying the MPM function, the RMSE values across the number of stream tubes do not indicate that increasing discretization improves model fit. Instead, the number of stream tubes that best fit observations varies with features of the cross-section and reach (Fig. 7). However, this result does not indicate that additional discretization is not useful for any applications of modeling sediment dynamics. Instead, the need for additional discretization should depend on the modeling objective and model capabilities.

Because parameters defining the channel hydraulics and sediment dynamics (e.g. depth, bed elevation, and downstream flow velocity and shear stress) in 1D models are averaged across the channel, these models are best suited to analysis at the reach-average level (Cui et al., 2008) where lateral sediment processes do not dominant erosion. One-dimensional models often cannot reliably simulate topographic features such as pools, riffles, and bars, nor location of a channel across a flat valley floor. They are often applied at a low spatial resolution, with cross-sections longitudinally spaced over several channel widths (Cui & Wilcox, 2008), leading to a smoothing of local topographic features. Thus, 1D models cannot simulate the 3D nature and sequence of widening and lateral erosional processes through terrace deposits that may be important drivers of rapid erosion of sediment from the reservoir (Grant et al., 2008). However, as a quasi-2D model based on the implementation of stream tubes, NETSTARS also cannot simulate the lateral erosion of sediment from the reservoir terraces and riverbanks or the lateral transfer of mass and momentum, and thus secondary flows. As a quasi-2D model, the flow and sediment transport characteristics are still treated as one-dimensional in each stream tube. While the number of fully morphodynamic 2D models available is growing, to our knowledge, only CONCEPTS (Langendoen & Simon, 2008) and SRH-2D (Lai et al., 2011) contain subroutines that address the geotechnical failure of banks that could simulate lateral erosion of terraces. An important area of research is in better integrating understanding on geotechnical bank failure (e.g. Osman & Thorne, 1988; Simon et al., 2000; Langendoen & Simon, 2008), longitudinal geomorphic dynamics (e.g. headcut migration; Stein & Julien, 1993), and existing conceptual models (e.g. Pizzuto, 2002) to facilitate identifying when lateral erosion of terraces is likely to be an important process (e.g. non-cohesive sediments, presence of seepage or tributaries through terrace, braided rivers, rapid dewatering, etc.) in reservoirs following dam removal.

However, simulating 2D erosional processes may not be necessary in every dam removal analysis. Some authors (Downs et al., 2009) have argued that the most realistic approach to modeling sediment pulses following dam removal is represented by 1D numerical simulation of reach-level channel changes. While it is possible that lateral erosion occurred during the first three months between dam failure and the first post-failure survey, as has been observed elsewhere (Major et al., 2012), it is not clear that lateral erosion was critical in shaping the channel response in the Dahan River where the entire valley cross-section is regularly mobilized during typhoons. We believe the sediment evacuation was dominated by very rapid headcut erosion, associated with the steep gradient of the Dahan River, local valley configuration, and high flows during the Weipa Typhoon.

The benefit of quasi-2D models is in the simulation of laterally-variable bed erosion, without direct representation of the processes (e.g. mass and momentum exchange) that occur in two dimensions. In our case study, we do not see conclusive evidence that increasing the number of stream tubes improved model fit to thalweg profiles or at individual cross-sections. However, it may be the case that, in wide, cross-sectionally variable channels with low valley gradients and low flow rates, quasi-2D models can more accurately simulate channel dynamics (Hsieh, 1996). We thus suggest that selection of the number of stream tubes should be based on the modeling objective as well as the channel and valley width, topographic variability, sinuosity, and sediment deposit properties as indications of the channel's potential to erode in a non-uniform manner.

Finally, the timescales of dominant sediment processes are also important in model accuracy. The NETSTARS model cannot directly simulate headcut processes, and thus results are not likely to be accurate for the short time scales over which rapid headcut migration occurs. However, NETSTARS, like other morphodynamic models, may be reasonably accurate over longer time scales as the channel adjusts following the passage of the headcut.

5. Conclusions

While not a deliberate removal, the failure of Barlin Dam released a pulse of sediment considerably larger than has occurred at the large majority of intentional dam removals, Advancing understanding on the sensitivities of mobile-bed models at Barlin Dam can support more informed modeling of future dam removals. To evaluate benefits of model configuration for sensitivity and fit to observation, we compared simulated and observed patterns of changes in elevation and volume associated with erosion and deposition along thalweg profiles and cross-sections. Our analyses illustrate that, in a steep river under high flows, this morphodynamic model was less sensitive to the spatial discretization of the cross-section than to the active layer thickness and sediment transport functions. Further, it appears that varying the reservoir active layer thickness over time may improve accuracy of predicted bed elevations. These results cast doubt on the benefits of universally increasing discretization for all applications in order to improve model fit, as average RMSE values of thalweg profiles did not decrease with increasing number of stream tubes.

Further sensitivity analyses should be conducted to investigate parameter interactions and uncertainty in field measurements and model parameterization. In addition, additional research should investigate whether multi-dimensional models perform better in river systems with lower gradients and under less extreme flows and identify the conditions under which lateral erosion of terraces is an important process to represent in dam removal cases.

References

Ackers, P., & White, W. R. (1973). Sediment Transport: A New Approach and Analysis. *Journal of the Hydraulics Division, ASCE*, *99*(11), 2041–2060.

Agriculture Engineering Research Center (2009). *Hydrological data of Shihmen Watershed*. Agriculture Engineering Research Center (*in Chinese*).

Barry, J. J., Buffington, J. M., & King, J. G. (2004). A general power equation for predicting bed load transport rates in gravel bed rivers. *Water Resources Research*, *40*(10).

Bennett, J. P., & Nordin, C. F. (1977). Simulation of sediment transport and armoring. *Hydrological Science Bulletin*, *4*(12), 555–570.

Cantelli, A., Paola, C., & Parker, G. (2004). Experiments on upstream-migrating erosional narrowing and widening of an incisional channel caused by dam removal. *Water Resources Research*, *40*(3), 1–12.

Cantelli, A., Wong, M., Parker, G., & Paola, C. (2007). Numerical model linking bed and bank evolution of incisional channel created by dam removal. *Water Resources Research*, *43*, 1–16.

Chang, C. H., Yang, J. C., & Tung, Y. K. (1993). Sensitivity and uncertainty analyses of a sediment transport model: a global approach. *Journal of Stochastic Hydrology and Hydraulics*, *7*(4), 299–314.
Chang, H. H. (2008). Case study of fluvial modeling of river responses to dam removal. *Journal of Hydraulic Engineering*, *134*(3), 295–302.
Cui, Y., Parker, G., Braudrick, C., Dietrich, W. E., & Cluer, B. (2006). Dam Removal Express Assessment Models (DREAM). Part 1: Model development and validation. *Journal of Hydraulic Research*, *44*(3), 291–307.
Cui, Y., & Wilcox, A. C. (2008). Sedimentation Engineering: Theory, Measurements, Modeling and Practice In: M. H. Garcia (Ed.), *Development and application of numerical modeling of sediment transport associated with dam removal* (pp. 995–1020). American Society of Civil Engineers.
Cui, Y., Wooster, J. K., Venditti, J. G., Dusterhoff, S. R., Dietrich, W. E., & Sklar, L. S. (2008). Simulating Sediment Transport in a Flume with Forced Pool-Riffle Morphology: Examinations of Two One-Dimensional Numerical Models. *Journal of Hydraulic Engineering*, *134*, 892–904.
Dadson, S. J., Hovius, N., Chen, H., Dade, W. B., Hsieh, M. L., Willett, S. D., & Lin, J. C. (2003). Links between erosion, runoff variability and seismicity in the Taiwan orogen. *Nature*, *426*, 648–651.
Downs, P. W., Cui, Y., Wooster, J. K., Dusterhoff, S. R., Booth, D. K., Dietrich, W. E., & Sklar, L. S. (2009). Managing reservoir sediment release in dam removal projects: An approach informed by physical and numerical modelling of non-cohesive sediment. *International Journal of River Basin Management*, *7*(4), 433–452.
Doyle, M. W., Stanley, E. H., & Harbor, J. M. (2002). Geomorphic Analogies for Assessing Probable Channel Response to Dam Removal. *Journal of the American Water Resources Association*, *38*(6), 1567–1579.
Emmett, W. W. (1980). A field calibration of the sediment-trapping characteristics of the Helley-Smith bedload sampler. *United States Geological Survey Professional Paper*, *1139*, 44.
Ferguson, R., & Church, M. (2009). A critical perspective on 1-D modeling of river processes: Gravel load and aggradation in lower Fraser River. *Water Resources Research*, *45*(11).
Gomez, B. (1991). Bedload transport. *Earth Science Reviews*, *31*(2), 89–132.
Gomez, B., & Church, M. (1989). An assessment of bedload sediment transport formulae for gravel bed rivers. *Water Resources Research*, *25*(6), 1161–1186.
Goode, J. R., & Wohl, E. (2010). Substrate controls on the longitudinal profile of bedrock channels: Implications for reach-scale roughness. *Journal of Geophysical Research*, *115*, F03018. http://dx.doi.org/10.1029/2008JF001188.
Grant, G., Marr, J., Hill, C., Johnson, S., Campbell, K., Mohseni, O., …Burkholder, B. (2008). Experimental and Field Observations of Breach Dynamics Accompanying Erosion of Marmot Cofferdam, Sandy River, Oregon. Proceedings of the World Environmental & Water Resources Congress, Honolulu, HI, USA, 12–16.
Hsieh, H. M. (1996). *Quasi-two Dimensional of Scour and Deposition in Alluvial Channels*. Taiwan: National Taiwan University Doctoral Dissertation.
Huang, J. S. (1994). *A Study of the Sustainable Water Resources System in Taiwan Considering the Problems of Reservoir Desilting* (p. 159) Taichung City, Taiwan: Taiwan Provincial Water Conservancy Bureau.
Hubbell, D. W. (1964). Apparatus and techniques for measuring bedload. *U.S. Geol. Surv. Water Supply Pap*, *1748*.
Hubbell, D. W. (1987). *Bed load sampling and analysis* (pp. 89–106)*New York*: *John Wiley and Sons* In *Sediment Transport in Gravel-bed Rivers*.
Kibler, K., Tullos, D., & Kondolf, M. (2011). Evolving Expectations of Dam Removal Outcomes: Downstream Geomorphic Effects Following Removal of a Small, Gravel-Filled Dam. *Journal of the American Water Resources Association*, *47*(2), 408–423.
Konrad, C. P. (2009). Simulating the recovery of suspended sediment transport and river-bed stability in response to dam removal on the Elwha River, Washington. *Ecological Engineering*, *35*(7), 1104–1115.
Lai, Y., Griemann, B., Sabatine, S., & Niemann, J. (2011). *Stream Bank Erosion, Turbidity Current, and Uncertainty Analysis: A Progress Report*. Denver, Colorado: USBR Technical Services Center USBR Technical Report No. SRH-2011-37.
Langendoen, E. J., & Simon, A. (2008). Modeling the Evolution of Incised Streams. II: Streambank Erosion. *Journal of Hydraulic Engineering*, *134*(7), 905–915.
Lee, H. Y., Hsieh, H. M., & Yang, C. T. (2003). *User's Manual for NETSTARS*.
Lee, H. Y., Hsieh, H. M., Yang, J. C., & Yang, C. T. (1997). Quasi two-dimensional simulation of scour and deposition in an Alluvial Channel. *Journal of Hydraulic Engineering*, *123*(3), 600–609.
Lisle, T. E., Cui, Y., Parker, G., Pizzuto, J. E., & Dodd, A. M. (2001). The dominance of dispersion in the evolution of bed material waves in gravel bed rivers. *Earth Surface Processes and Landforms*, *26*(13), 1409–1420.
Major, J. J., O'Connor, J. E., Podolak, C. J., Keith, M. K., Grant, G. E., Spicer, K. R., & Wilcock, P. R. (2012). Geomorphic response of the Sandy River, Oregon, to removal of Marmot Dam. *U.S. Geological Survey Professional Paper*, *1792*, 64.
McLean, D. G. (1985). Sensitivity analysis of bedload equations. Proceedings Canadian Society for Civil Engineering Annual Conference, Saskatoon, Sask, 1–15.
Milliman, J. D., & Syvitski, P. M. (1992). Geomorphic/tectonic control of sediment discharge to the ocean: the importance of small mountainous rivers. *Journal of Geology*, *100*(5), 525–544.
Morris, G. L., & Fan, J. (1998). *Reservoir Sedimentation Handbook*. New York: McGraw-Hill.
Newham, L. T. H., Norton, J. P., Prosser, I. P., Croke, B. F. W., & Jakeman, A. J. (2003). Sensitivity analysis for assessing the behaviour of a landscape-based sediment source and transport model. *Environmental Modelling and Software*, *18*, 741–751.
Osman, A. M., & Thorne, C. R. (1988). Riverbank stability analysis. I: Theory. *Journal of Hydraulic Engineering*, *114*(2), 134–150.
Pizzuto, J. (2002). Effects of Dam Removal on River Form and Process. *BioScience*, *52*(8), 683–691.
Rathburn, S., & Wohl, E. (2003). Predicting fine sediment dynamics along a pool-riffle mountain channel. *Geomorphology*, *55*(1), 111–124.
Ruark, M. D., Niemann, J. D., Greimann, B. P., & Arabi, M. (2011). Method for assessing impacts of parameter uncertainty in sediment transport modeling applications. *Journal of Hydraulic Engineering*, *137*(6), 623–636.
Rulot, F., Dewals, B. J., Erpicum, S., Archambeau, P., & Pirotton, M. (2012). Modelling sediment transport over partially non-erodible bottoms. *International Journal for Numerical Methods in Fluids*, *70*(2), 186–199.
Simon, A., Curini, A., Darby, S. E., & Langendoen, E. J. (2000). Bank and near-bank processes in an incised channel. *Geomorphology*, *35*(3), 193–217.
Simons, D. B., & Şentürk, F. (1992). *Sediment Transport Technology: water and sediment dynamics*. Littleton, Colorado: Water Resources Publications.
Stein, O. R., & Julien, P. Y. (1993). Criterion delineating the mode of headcut migration. *Journal of Hydraulic Engineering*, *119*(1), 37–50.
Stock, J. D., Montgomery, D. R., Collins, B. D., Dietrich, W. E., & Sklar, L. (2005). Field measurements of incision rates following bedrock exposure: Implications for process controls on the long profile of valleys cut by rivers and debris flows. *Geological Society of America Bulletin*, *117*(11/12), 174–194.
Struiksma, N. (1999). Mathematical modelling of bedload transport over non-erodible layers. In Proceedings of IAHR Symposium on River, Coastal and Estuarine Morphodynamics, Genova, 1, 89–98.
Tullos, D., Cox, M., & Walter, C. (2010). Simulating dam removal with a 1D hydraulic model: Accuracy and techniques for reservoir erosion and downstream deposition at the Chiloquin Dam removal. In Proceedings of the 2010 ASCE Environmental and Water Resources Institute conference, Providence, RI, pp. 1737–1749.
Tullos, D., & Wang, H. W. (2014). Morphological Responses and Sediment Processes following a Typhoon-induced Dam failure, Dahan River, Taiwan, China. *Earth Surface Processes and Landforms*, *39*(2), 245–258.
Water Resources Agency (2007). *Preliminary Investigation of Barlin Dam Failure*. Water Resources Agency, Taiwan in Chinese.
Water Resources Agency (2008b). *Management and Planning Report for Dahan River*. Taiwan, China: Water Resources Agency in Chinese.
Wells, R. R., Langendoen, E., & Simon, A. (2007). Modeling pre and post removal sediment dynamics: The Kalamazoo River, Michigan. *Journal of the American Water Resources Association*, *43*(3), 773–785.
Wilcock, P. R., Barta, A. F., Shea, C. C., Kondolf, G. M., Matthews, W. G., & Pitlick, J. (1996). Observations of Flow and Sediment Entrainment on a Large Gravel-Bed River. *Water Resources Research*, *32*(9), 2897–2909. http://dx.doi.org/10.1029/96WR01628.
Williams, D. T., & Julien, P. Y. (1989). Applicability index for sand transport equations. *Journal of Hydraulic Engineering*, *115*(1), 1578–1581.
Wu, W. (2004). Depth-Averaged Two-Dimensional Numerical Modeling of Unsteady Flow and Nonuniform Sediment Transport in Open Channels. *Journal of Hydraulic Engineering*, *130*(100), 1013–1024.
Yang, C. T. (1973). Incipient Motion and Sediment Transport. *Journal of the Hydraulics Division*, *99*(10), 1679–1704.
Yang, C. T. (2006). *Erosion and Sedimentation Manual*. Technical Service Center, US Bureau of Reclamation Denver, Colorado.
Yang, C. T. (2008). GSTARS Computer Models and Sedimentation Control in Surface Water Systems. In The 3rd International Conference on Water Resources and Arid Environments.
Yang, C. T., & Young, C. A. (1997). *Major Sediment Issues Confronting the Bureau of Reclamation and Research Needs towards Resolving these Issues*. Proceedings of the U.S. Geological Survey (USGS) Sediment Workshop In.

Further reading

Cao, Z., & Carling, P. A. (2003). On evolution of bed material waves in alluvial rivers. *Earth Surface Processes and Landforms*, *28*(4), 437–441.
Cao, Z., Pender, G., Wallis, S., & Carling, P. (2004). Computational dam-break hydraulics over erodible sediment bed. *Journal of Hydraulic Engineering*, *130*(7), 689–703.
Cui, Y., Parker, G., Lisle, T. E., Pizzuto, J. E., & Dodd, A. M. (2005). More on the evolution of bed material waves in alluvial rivers. *Earth Surface Processes and Landforms*, *30*(1), 107–114.
Evans, J. (2007). Sediment impacts of the 1994 Failure of IVEX dam (Chagrin River, NE Ohio): A Test of channel evolution models. *Journal of Great Lakes Research*, *33*, 90–102.
Gomez, B., & Phillips, J. D. (1999). Deterministic Uncertainty in Bed Load Transport. *Journal of Hydraulic Engineering*, *125*(3), 305–308.
Lisle, T. E., Pizzuto, J. E., Ikeda, H., Iseya, F., & Kodama, Y. (1997). Evolution of a sediment wave in an experimental channel. *Water Resources Research*, *33*(8), 1971–1981.
Madej, M. A. (2001). Development of channel organization and roughness following sediment pulses in single-thread, gravel bed rivers. *Water Resources Research*, *37*(8), 2259–2272.
Meyer-Peter, E., & Muller, R. (1948). Formulas for Bedload Transport. 2nd IAHR congress, Stockholm, 39–64.

Shei-Pa National Park (2010). *Numerical Simulations and Physical Modeling of Potential Sediment Impact Assessment and Dam Removal Strategies for the No. 1 Check Dam on Chijiawan Creek.).* Shei-pa National Park in Chinese.
Water Resources Agency (2006). *Evaluation Study of Landslide Susceptibility and Landslide Size in Reservoir Watersheds*. Taiwan: Water Resources Agency in Chinese.
Water Resources Agency (2008a). *Field Investigation on Barlin Dam reach*. Taiwan, China: Water Resources Agency in Chinese.
Wilcock, P. R. (1996). Estimating local bed shear stress from velocity observations. *Water Resources Research*, *32*(11), 3361–3366.